ACS Energy LETTERS

http://pubs.acs.org/journal/aelccp

Spatial Management of CO Diffusion on Tandem Electrode Promotes NH_2 Intermediate Formation for Efficient Urea Electrosynthesis

Yan Wang,[‖] Shuai Xia,[‖] Jianfang Zhang,* Zhengyuan Li, Rui Cai, Cuiping Yu, Yong Zhang, Jingjie Wu,* and Yucheng Wu*

Cite This: *ACS Energy Lett.* 2023, 8, 3373−3380

Read Online

ACCESS | Metrics & More | Article Recommendations | Supporting Information

ABSTRACT: **Electrocatalytic urea synthesis is a promising alternative to the energy-intensive conventional industrial process. However, it lacks highly active and selective catalyst systems. Herein, we report a Cu/ZnO stacked tandem gas-diffusion electrode (GDE) for selective urea synthesis from electrocatalytic CO_2 and nitrate reduction reactions. The ZnO catalyst layer (CL) segment at the inlet provides a high CO concentration to the downstream Cu CL segment, promoting the conversion of NO_3^- to $*NH_2$. The CO-mediated NH_2 formation accelerates the C−N coupling rate for urea synthesis. As a result, the stacked GDE with an optimal ZnO/Cu CL area ratio achieves a high Faradaic efficiency of 37.4% and a high yield of 3.2 μmol h^{-1} cm^{-2} for urea at −0.3 V vs RHE under ambient conditions. This work expands the application of tandem electrodes and realizes the cascade C−N coupling reaction.**

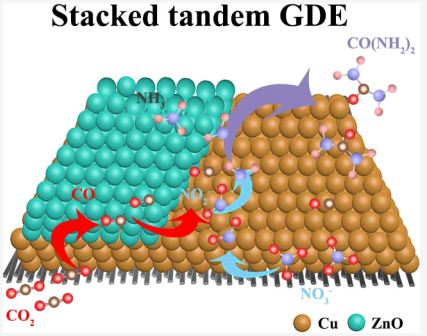

Urea is one of the important nitrogen-based fertilizers in agricultural production.[1] Currently, the industrial production of urea is operated by reducing carbon dioxide (CO_2) and ammonia (NH_3) under harsh conditions.[2,3] This industrial technology requires a series of complex manufacturing, storage, and transportation processes, resulting in huge energy consumption. In particular, a lot of energy is wasted during the transportation process.[4] Therefore, an urgent need is to explore an alternative technology for decentralized urea production using clean energy.[5,6] Renewable electrical energy-powered electrocatalysis can be a promising route for urea synthesis by reducing CO_2 and nitrogen-containing molecules.[7−10]

The nitrogen-containing reactants for urea electrosynthesis include NH_3, N_2, oxynitride (NO_x), and nitrate/nitrite (NO_3^-/NO_2^-).[11−17] The NH_3 is mainly produced by the industrial Haber−Bosch process, which requires high energy input and emits 1.9 tons of CO_2 per ton of NH_3.[18] The activation of N_2 is still challenging due to the high bond energy of N≡N (941 kJ mol^{-1}), limiting further reduction.[19,20] The biotoxicity of NO_x hinders its direct application in urea electrosynthesis.[21] By contrast, their hydrates (NO_3^-/NO_2^-) have been used as nitrogen sources to couple with CO_2 reduction for effective urea electrosynthesis.[22−26] However, by coupling with CO_2, the NO_3^--to-urea route involves complex multistep proton-coupled electron-transfer steps, still suffering from low Faradaic efficiency and current density.[24,27] The high energy barrier for the C−N coupling restricts the efficiency of the electrosynthesis of urea. Designing a highly active catalyst system is key to accelerating the kinetics of the C−N coupling reaction in urea electrosynthesis.

The coupling reaction between $*CO$ and $*NH_2$ intermediates is considered the rate-determining step (RDS) step of C−N bond formation in urea synthesis.[28,29] The kinetics of the C−N coupling reaction depends on the adsorption strength of $*CO$ and $*NH_2$ on the catalytic sites and their surface coverages.[30,31] The high surface coverage of $*CO$ (θ_{*CO}) and $*NH_2$ (θ_{*NH2}) is conducive to increasing the C−N coupling rate.[32] Increasing local concentrations of $*CO$ and $*NH_2$ intermediates near the catalyst surface enhances θ_{*CO} and θ_{*NH2}.[33−35] Therefore, the yield of urea can be improved by increasing the local CO and NH_2 concentrations. For a single catalyst, the excess generation of either $*CO$ or $*NH_2$ intermediate will hinder the adsorption of the other intermediate at the active site, resulting in a low C−N coupling rate.[36] The cascade system for electrocatalytic urea

Received: April 20, 2023
Accepted: July 5, 2023
Published: July 14, 2023

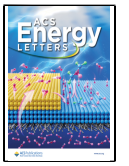

https://doi.org/10.1021/acsenergylett.3c00824
ACS Energy Lett. 2023, 8, 3373−3380

synthesis decouples the *CO and *NH_2 formation via two parallel steps of CO_2-to-CO and NO_3^--to-NH_2 occurring at two different catalytic sites.[37] That is to say, one catalyst with CO-selective sites supplies sufficient CO, and another can effectively convert NO_3^- to NH_2.[38] It also requires enabling C−N coupling on either a CO-selective site or a NH_2-selective site.

Our previous studies have demonstrated that a tandem gas-diffusion electrode (GDE) dramatically improves the production rate of multicarbon products from CO_2 reduction through spatial management of CO transport.[39−41] In a stacked tandem GDE, the local concentration of CO intermediate can be finely managed along the length of the Cu CL.[41] The success of tandem GDEs in the electrocatalytic conversion of CO_2-to-multicarbon products encouraged us to explore further the potential of these tandem GDE structures in other electrocatalytic reactions. In addition, a recent study revealed that the CO intermediate generated by CO_2 reduction accelerates hydrodeoxidation of *NO_x intermediates to form *NH_2.[42] We hypothesize that concentrated CO at the inlet of stacked tandem GDE could promote *NH_2 formation and thus enhance θ_{*NH2} at the Cu CL, improving the kinetics of C−N coupling between *CO and *NH_2 intermediates.

Herein, we adopt the design of structurally stacked tandem GDE to synthesize urea by selective co-reduction of CO_2 and NO_3^-. ZnO-based catalysts exhibit superior catalytic activity for electrocatalytic CO_2-to-CO.[43,44] Cu-based catalysts can provide highly active sites for NH_3 (or *NH_2) synthesis by reducing N_2, NO_3^-, and NO_2^-.[45,46] The stacked GDE integrates a CO-selective ZnO CL segment with a NH_2-selective Cu CL segment. The concentration distribution of the *CO and *NH_2 intermediates was managed spatially by rationally arranging the area ratio of the Cu and ZnO segments. The C−N coupling rate was accelerated by enhancing θ_{*CO} and θ_{*NH2} simultaneously. The optimal stacked $Cu_{1.0}/Zn_{0.5}$ GDE with a Cu:ZnO area ratio of 1.0:0.5 achieved a high yield of 3.2 μmol h^{-1} cm^{-2} and a high FE of 37.4% for urea at a potential of −0.3 V (vs RHE, thereafter) in a flow cell electrolyzer. In situ Raman and attenuated total reflection Fourier transform infrared (ATR-FTIR) analysis revealed that the *CO intermediate facilitated the reduction of NO_3^- to the *NH_2 intermediate and promoted the formation of the C−N bond in urea synthesis.

In the urea synthesis process, the distribution of reaction intermediates such as *CO from CO_2 reduction and *NH_2 from NO_3^- reduction plays a crucial role in the cascade C−N coupling rate. We employed tandem GDEs to tune the electrode's spatial concentrations of *CO and *NH_2. The Cu catalyst for NO_3^--to-NH_3 reduction and the ZnO catalyst for CO_2-to-CO reduction were chosen to construct tandem GDEs with separated Cu and ZnO segments, as shown in Figure 1a. In a flow cell reaction system, CO generated by ZnO at the inlet flowed downstream the Cu CL, promoting the hydrodeoxidation of NO_3^- to *N intermediates and then to *NH_2 intermediates.[42] Previous work suggested that the urea was produced by the C−N coupling of *CO and *NH_2 intermediates: *CO + 2*NH_2→ $CO(NH_2)_2$.[25,38] The generation rate of urea (r_{urea}) is determined by the RDS kinetics: $r_{urea} = k[*CO][*NH_2]^2$. Because of positive reaction orders with respect to both θ_{*CO} and θ_{*NH2}, the reaction rate of C−N coupling could be increased by enhancing θ_{*CO} and θ_{*NH2} on the catalyst surface. In the stacked GDE, the upstream ZnO CL offers a high local CO concentration at the inlet (Figure 1b). The concentrated CO translates to a high θ_{*CO}. The high θ_{*CO} facilitates the reduction of NO_3^- to *NH_2 at the Cu sites, leading to a high θ_{*NH2}, which in turn promotes the C−N coupling reaction toward urea production. Compared with a conventional pure Cu GDE, the stacked GDE enhances CO and NH_2 conversion due to the prolonged residence time.

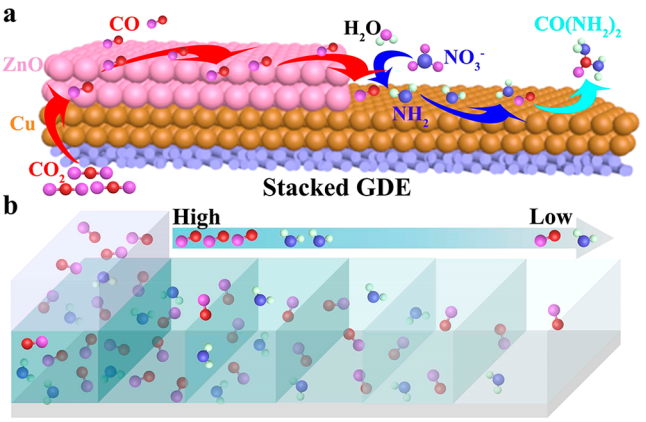

Figure 1. Concept of urea synthesis on stacked tandem GDE. (a) Schematic illustration of stacked Cu/ZnO GDE. (b) Variation of *CO and *NH_2 intermediates concentration along the length of Cu CL.

A series of stacked Cu/ZnO GDEs were designed by progressively shrinking the ZnO CL areas (Figure 2a,b). The mass of ZnO was kept at 0.05 mg in all stacked GDEs, while the loading varied with the segment area. Since the mass of the ZnO segment was constant, the thickness of ZnO CL decreased as the ZnO segment area increased. The ZnO CL in the $Cu_{1.0}/ZnO_{0.2}$ GDE has the largest thickness of 3.5 μm (Figure S1), causing the highest diffusion resistance. In contrast, the thickness of ZnO CL in the $Cu_{1.0}/ZnO_{0.5}$ GDE decreases to 1.2 μm (Figure 2c). Such a thin ZnO CL was sufficient to conquer the mass transport limitations and maximize active site exposure.

The electrocatalytic CO_2 and NO_3^- reduction was conducted in a flow cell using a 0.1 M KNO_3 electrolyte. CO_2 was fed into the gas channel of the reactor at a flow rate of 20 sccm. The absorbances of urea were detected by UV−vis spectroscopy after 1 h of electrocatalysis (Figure S2). The generated urea was quantified by the diacetyl monoxime method using a calibration curve (Figure S3). The amounts of byproducts, including NO_2^-, NH_3, and N_2H_4, were also measured by UV−vis spectra based on their corresponding calibration curves (Figures S4−S8). The yields and FEs of urea, NO_2^-, and NH_3 at different potentials are displayed in Figures S9−S11. No N_2H_4 was detected by UV−vis spectroscopy (Figure S12). Besides, the outlet gas products and the liquid products of CO_2 reduction were quantified by online gas chromatography (GC) and ^1H nuclear magnetic resonance (NMR) spectroscopy, respectively. The CO partial current density (j_{CO}) and corresponding FE were calculated and compared among different stacked Cu/ZnO GDEs and pure Cu GDE (Figures S13 and S14). Figure 2d compares the yield and FE of urea among four types of stacked Cu/ZnO GDEs and pure Cu GDE at −0.3 V. Both the yield and FE first increased with the area ratio increase from 1.0:0.2 to 1.0:0.5 and then dropped with the further increase of ZnO CL area. The $Cu_{1.0}/ZnO_{0.5}$ GDE achieved the highest urea yield of 3.2

https://doi.org/10.1021/acsenergylett.3c00824
ACS Energy Lett. 2023, 8, 3373−3380

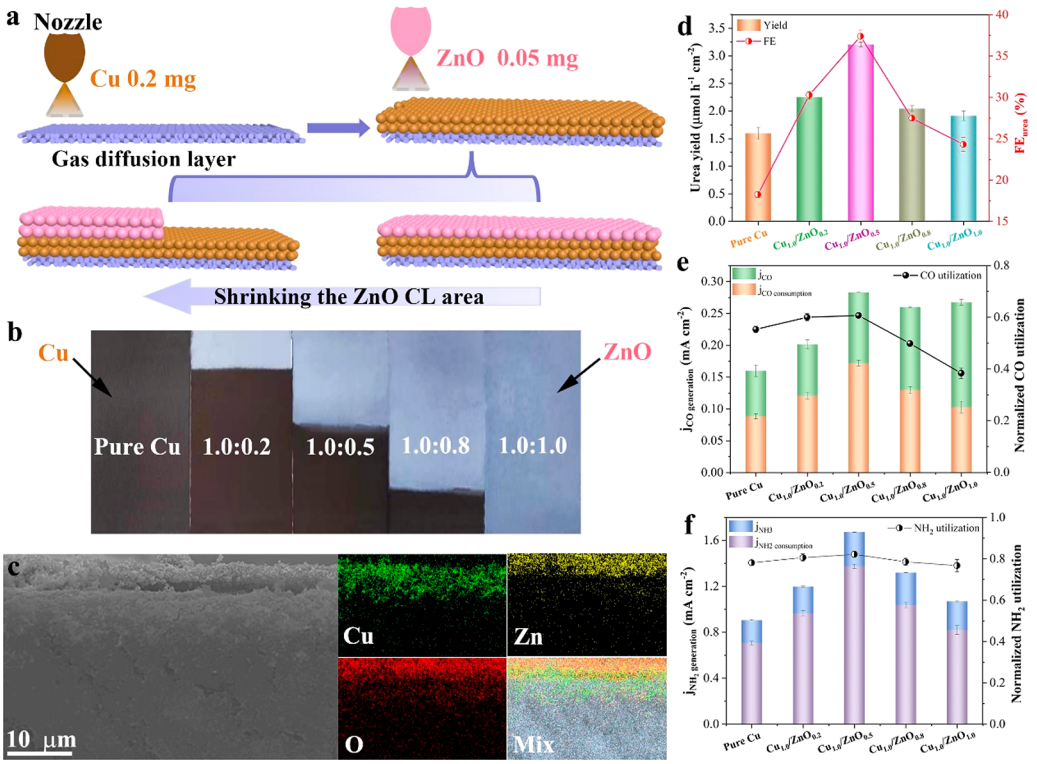

Figure 2. Preparation and performance of the stacked Cu/ZnO GDEs. (a) Schematic of the preparation process. (b) Photographs of the stacked Cu/ZnO GDEs with different Cu to ZnO area ratios. (c) Cross-section SEM and corresponding EDS mapping images of the stacked $Cu_{1.0}/ZnO_{0.5}$ GDE. (d) The yields and FEs of urea produced on different stacked Cu/ZnO GDEs at −0.3 V. (e) Values of $j_{CO\ generation}$ and corresponding normalized CO utilization for different stacked Cu/ZnO GDEs at −0.3 V. (f) Values of $j_{NH2\ generation}$ and corresponding normalized NH_2 utilization for different stacked Cu/ZnO GDEs at −0.3 V.

μmol h^{-1} cm^{-2} at −0.3 V, 2-fold that of pure Cu GDE. The FE of urea was significantly improved by stacking the ZnO CL onto Cu CL and reached a maximum value of 37.4% at −0.3 V on the $Cu_{1.0}/ZnO_{0.5}$ GDE. The yield and FE of urea from the stacked $Cu_{1.0}/ZnO_{0.5}$ GDE were also higher than those of some reported catalysts (Table S1). The improved performance of the stacked Cu/ZnO GDE is mainly attributed to the spacial CO concentration well-managed along the Cu CL, as reflected by the performance of the control electrodes. The mixed Cu/ZnO GDE performs the CO_2-to-CO conversion on the scattered ZnO over the whole GDE, leading to disordered and dispersed CO distribution. The resulting low CO concentration leads to insufficient NO_3^- to NH_2 conversion and lowers the urea yield (Figure S15). A coplanar $Cu_{0.5}/ZnO_{0.5}$ GDE governs the CO flow only along the downstream Cu CL without crossing the underneath Cu CL, making the CO diffusion differ from the stacked structure. Although a similar CO generation as the stacked structure, inadequately exposed active Cu sites on the shrunken Cu CL in a coplanar GDE slow down the C−N coupling rate (Figure S16). In addition, the urea yield and FE of a reversed stacked $ZnO_{1.0}/Cu_{0.5}$ GDE were much lower than those of the stacked $Cu_{1.0}/ZnO_{0.5}$ GDE (Figure S17).

The concentration and distribution of two key intermediates, CO and NH_2, are compared among the stacked Cu/ZnO GDEs. Both CO and NH_2 utilizations are defined as the ratio of the consumption rate to the generation rate. The generation rate of CO or NH_2 ($j_{CO\ generation}$ or $j_{NH2\ generation}$) represents the sum of the CO or NH_2 consumption rate ($j_{CO\ consumption}$ or $j_{NH2\ consumption}$) for urea synthesis and the remaining CO or NH_2 current density (j_{CO} or j_{NH2}). As revealed in Figure 2e,f, both $j_{CO\ consumption}$ and $j_{NH2\ consumption}$ show a volcano shape concerning the ZnO CL area, consistent with the trend of urea yield. This convergence indicates that rapid CO and NH_2 intermediates consumption translates to a fast C−N coupling rate. Although the conductivity of Cu/ZnO GDEs decreased with the increase of ZnO CL area (Figure S18), it has little effect on the urea yield due to the almost equal amount of CO produced from the ZnO CL. Since the ZnO CL facilitated the reduction of CO_2 to CO, the value of $j_{CO\ generation}$ increased nearly twice in the $Cu_{1.0}/ZnO_{0.5}$ GDE compared with the pure Cu GDE and remained almost the same as in both the $Cu_{1.0}/ZnO_{0.8}$ GDE and $Cu_{1.0}/ZnO_{1.0}$ GDE. However, the $j_{CO\ generation}$ of the $Cu_{1.0}/ZnO_{0.2}$ GDE was only slightly higher than that of pure Cu GDE due to the mass-transport limitation of thicker ZnO CL and deficiently exposed ZnO active sites. As a result, the urea yield slightly increases for the $Cu_{1.0}/ZnO_{0.2}$ GDE. The R_{ct} values of the co-reduction of CO_2 and NO_3^- for pure Cu and $Cu_{1.0}/ZnO_{0.2}$ GDEs differed from those of hydrogen evolution reaction (HER) in the absence of CO_2 and NO_3^- (Figure S19). The reciprocal R_{urea} (R_{urea}^{-1}) reflects the reaction rate of urea synthesis. The ratio $R_{urea}^{-1}/(R_{urea}^{-1} + R_{HER}^{-1})$ for the $Cu_{1.0}/ZnO_{0.2}$ GDE was higher than that of pure Cu, indicating that adding ZnO suppresses HER.

Notably, the $Cu_{1.0}/ZnO_{0.5}$ GDE exhibited the highest CO utilization, as determined by $j_{CO\ consumption}/j_{CO\ generation}$. Adsorbed *CO near the $*NO_3$ adsorption site promotes the cleavage of the nitrogen oxidation bond by reducing the deoxygenation energy barrier.[42] Meanwhile, the $Cu_{1.0}/ZnO_{0.5}$ GDE also showed the highest $j_{NH2\ generation}$. Higher local θ_{*CO} could accelerate the deoxygenation of $*NO_3$ to *N and the subsequent hydrogenation reaction to generate $*NH_2$

https://doi.org/10.1021/acsenergylett.3c00824
ACS Energy Lett. 2023, 8, 3373−3380

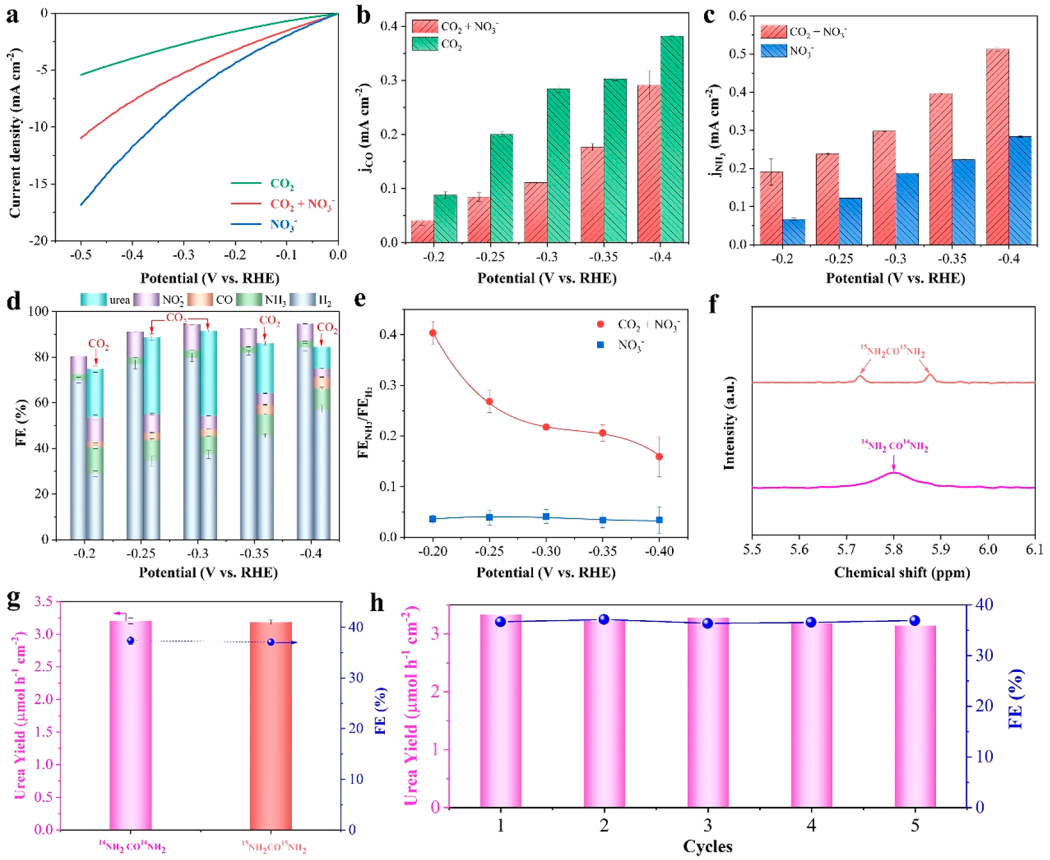

Figure 3. Electrochemical performance of the stacked $Cu_{1.0}/ZnO_{0.5}$ GDE. (a) Linear sweep voltammetry curves. (b) Compared j_{CO} for CO_2 reduction with and without NO_3^-. (c) Compared j_{NH3} for NO_3^- reduction with and without CO_2. (d) FEs of the main products in KNO_3 with and without CO_2. (e) FE ratios of NH_3 to H_2 in KNO_3 with and without CO_2. (f) ^1H NMR spectra of urea produced from $^{14}NO_3^-$ + CO_2 and $^{15}NO_3^-$ + CO_2. (g) Corresponding yield and FE of urea quantified by ^1H NMR. (h) Yield and FE of five independent cycling tests at −0.3 V.

intermediates. As a result, the largest $j_{NH2\ generation}$ (or highest θ_{*NH2}) was obtained on the $Cu_{1.0}/ZnO_{0.5}$ GDE. The increased local θ_{*NH2} contributes to extensive $*NH_2$ utilization for urea synthesis. The role of CO concentration on the urea yield can be further uncovered by feeding CO_2 and CO mixture gas (Figure S20). The urea yield and FE for the pure Cu GDE increased accordingly with the increase of CO percentage in the mixture gas. The above results indicated that stacked $Cu_{1.0}/ZnO_{0.5}$ GDE possessed the largest θ_{*CO} and θ_{*NH2}, leading to the highest yield and selectivity of urea among these GDEs.

We then focused on the facilitating effect of CO_2 reduction on the urea synthesis from the stacked $Cu_{1.0}/ZnO_{0.5}$ GDE. Linear sweep voltammetry (LSV) was carried out to preliminarily assess the performance of the $Cu_{1.0}/ZnO_{0.5}$ GDE in different reaction conditions. As shown in Figure 3a, the total current density was the lowest in 0.1 M $KHCO_3$ electrolyte with CO_2 feeding gas while significantly increased in 0.1 M KNO_3 electrolyte, indicating the faster reaction kinetics of NO_3^- reduction than CO_2 reduction. The current density of coelectrolysis of 0.1 M KNO_3 and CO_2 was lower than the electrolysis of 0.1 M KNO_3 alone. The decrease in current density can be attributed to the suppression of HER by CO_2.[15] Similar phenomena were also observed in chronoamperometric tests in 0.1 M KNO_3 with and without CO_2 (Figure S21). The partial current densities of CO and NH_3 were calculated to explore further the role of CO_2 in urea synthesis (Figure 3b,c). The j_{CO} of CO_2 reduction alone was higher than that of coelectrolysis of CO_2 and NO_3^-, suggesting that CO was consumed for urea synthesis. Inversely, the j_{NH3} of CO_2 and NO_3^- co-reduction increased nearly twice that of sole NO_3^- reduction. It implies that *CO generated by CO_2 reduction promotes the NO_3^- reduction to NH_3 by accelerating the cleavage of N−O bonds and extracting the O from *NO.[42,47] As shown in Figure 3d, in the absence of CO_2, the FE of NH_3 was less than 3.5%, while the FE of H_2 reached above 80% at −0.3 V. Upon feeding CO_2, the FE of NH_3 increased to about 8%, and the FE of H_2 decreased dramatically to 40% at the same potential. The FE ratio of NH_3 to H_2 was significantly enhanced in the KNO_3 electrolyte with CO_2 feeding, 11 times higher than that of pure KNO_3 at −0.2 V (Figure 3e). Thus, CO_2 enables urea synthesis by promoting NO_3^- reduction and suppressing HER.

The source of nitrogen in urea synthesis was determined by ^{15}N isotope labeling. As shown in Figure 3f, the $CO(^{14}NH_2)_2$ derived from $K^{14}NO_3$ has only one peak in the ^1H NMR spectrum. In contrast, typical double peaks are presented in the ^1H NMR spectrum for $CO(^{15}NH_2)_2$ made from $K^{15}NO_3$.[48] The ^1H NMR spectra confirmed that the nitrogen source of urea originated from electrocatalytic NO_3^- reduction. Moreover, the calculated yield and FE of both $CO(^{15}NH_2)_2$ and $CO(^{14}NH_2)_2$ by ^1H NMR are close to those quantified by the diacetyl monoxime method (Figure 3g). It is worth pointing out that no urea was generated from the reaction of NH_3 and

https://doi.org/10.1021/acsenergylett.3c00824
ACS Energy Lett. 2023, 8, 3373−3380

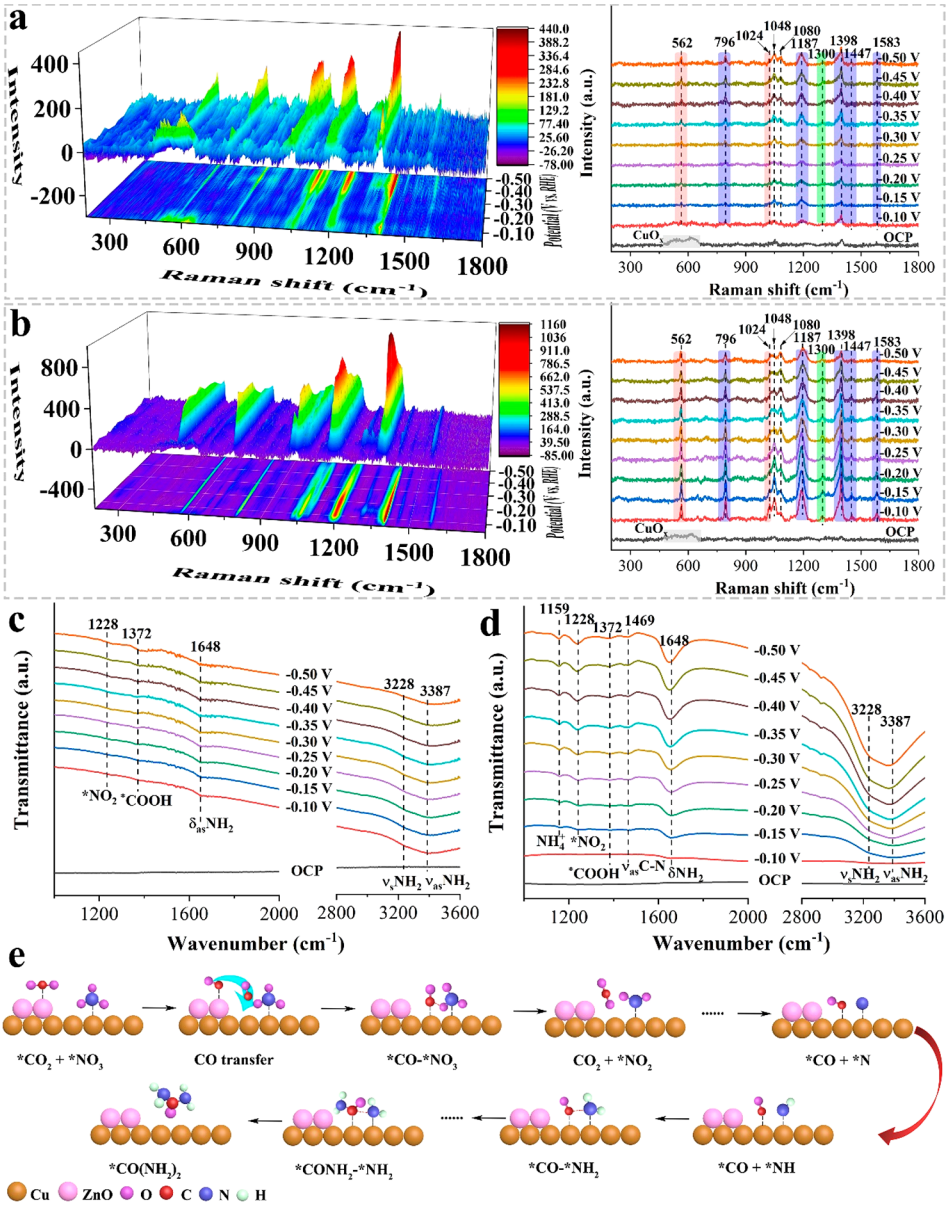

Figure 4. Reaction mechanism of urea synthesis on the stacked tandem GDE. In situ Raman spectra of (a) pure Cu GDE and (b) $Cu_{1.0}$/$ZnO_{0.5}$ GDE. In situ ATR-FTIR spectra of (c) pure Cu GDE and (d) $Cu_{1.0}$/$ZnO_{0.5}$ GDE. (e) Proposed mechanism of CO-mediated NO_3^- reduction for urea synthesis. For simplicity, only the Cu site in the downstream segment is shown to readsorb CO and enable C−N coupling. Note that the Cu sites over the whole segments participate in the reactions.

CO_2 over Cu/ZnO electrodes with or without an applied potential (Figure S22), further supporting that urea was produced by electrocatalytic co-reduction of NO_3^- and CO_2 rather than the chemical reaction of NH_3 and CO_2-derived carbamate salt in the electrolyte.

The stability of electrocatalytic urea synthesis was investigated by performing five independent cycle tests on the $Cu_{1.0}$/$ZnO_{0.5}$ GDE (Figures S23 and S24). A constant potential of −0.3 V was applied at each 1 h cycle. Figure 3h shows that both yield and FE of urea have no noticeable decline after 5 cycles. The in situ Raman spectra of the $Cu_{1.0}$/$ZnO_{0.5}$ GDE revealed that the surface ZnO was reduced to Zn as the potential was swept negatively (Figure S25). The XRD results showed that the ZnO phase in the $Cu_{1.0}$/$ZnO_{0.5}$ electrode could remain well after different reaction times (Figure S26), suggesting that only the ZnO scale was in situ reduced to metallic Zn, aligning with the XPS spectra results (Figure S27).

To elucidate the reaction mechanism of urea synthesis from cascade of CO_2 and NO_3^- reduction, in situ Raman spectroscopy was performed to monitor the surface-adsorbed intermediates during the reaction. Some common reaction intermediates were detected in the in situ Raman spectra of the pure Cu GDE and $Cu_{1.0}$/$ZnO_{0.5}$ GDE (Figure 4a,b), signifying the same reaction pathway for urea synthesis. Under an open circuit potential (OCP), the Cu oxides appeared at 500−650 cm^{-1}, and adsorbed species of NO_3^- and CO_3^{2-} emerged at 1048 and 1080 cm^{-1}, respectively. When the applied potential shifted negatively, the Raman peak of CH_2 bending vibration (δCH_2) from CO_2 reduction was observed at 1300 cm^{-1}.[49] The N-containing intermediates from NO_3^- reduction appeared at 796, 1187, 1398, 1447, and 1583 cm^{-1},

https://doi.org/10.1021/acsenergylett.3c00824
ACS Energy Lett. 2023, 8, 3373−3380

corresponding to the bending vibration of NO_2^- (δNO_2^-), symmetrical vibration of NO_2^- ($\nu_s NO_2^-$), $\delta_s NH_2$ deformation, symmetrical bending vibration of NH_3^+ ($\delta_s NH_3^+$), and $\delta_{as} NH_2$ of NH_3, respectively.[49,50] Besides, the δ(CN) and ν_s(CN) bonds were also found at 562 and 1024 cm^{-1}, demonstrating the formation of urea.[51,52] The peak intensities of these reaction intermediates adsorbed on the surface of $Cu_{1.0}/ZnO_{0.5}$ GDE were higher than those on pure Cu GDE as well as $Cu_{1.0}/ZnO_{1.0}$ GDE (Figure S28). Notably, the intermediate adsorption was detected over the whole electrode, including the interface between Cu and ZnO segments (Figure S29), which proves that the whole Cu segment participates in the C−N coupling for urea synthesis.

The reaction intermediates on the pure Cu and stacked Cu/ZnO GDEs were further identified by in situ ATR-FTIR spectroscopy (Figure 4c,d and Figure S30). Four obvious vibration bands from NO_3^- reduction appeared at about 1228, 1648, 3228, and 3387 cm^{-1}, which could be ascribed to the adsorbed $*NO_2$, N−H bending vibration of NH_2 (δNH_2), and N−H stretching vibration of NH_2 ($\nu_s NH_2$ and $\nu_{as} NH_2$), respectively.[15,26,31,53] The band of adsorbed *COOH intermediates at 1372 cm^{-1} was generated from CO_2 reduction.[12,28] Compared to pure Cu GDE, two new peaks arose at 1159 and 1469 cm^{-1}, respectively, corresponding to the vibration of NH_4^+ and the asymmetrical vibration of the C−N bond in urea.[7,31] The intensities of $*NO_2$, $*NH_2$, and $*NH_4^+$ adsorbed on the surface of $Cu_{1.0}/ZnO_{0.5}$ GDE increased dramatically as the potential shifted negatively. The intensities of these N-containing intermediates on the surface of $Cu_{1.0}/ZnO_{0.5}$ GDE were much higher than those on pure Cu and $Cu_{1.0}/ZnO_{1.0}$ GDEs (Figure S30), further demonstrating that in situ-generated *CO enhanced NO_3^- reduction on the surface of $Cu_{1.0}/ZnO_{0.5}$ GDE.

Based on in situ spectroscopy results, we proposed that intensifying CO could promote the hydrodeoxygenation of $*NO_3^-$ to $*NH_2$, thus accelerating the C−N coupling rate for urea synthesis (Figure 4e). The cascade C−N coupling reaction integrates two parallel steps of CO_2-to-CO and NO_3^--to-NH_2 on two distinct catalytic sites in a tandem GDE. In the stacked Cu/ZnO GDE, *CO adsorbed on the ZnO site would extract the O from $*NO_3^-$ adsorbed on the Cu site nearby, facilitating the cleavage of the N−O band. In the deoxygenation step, *CO contributed to the decomposition of N−O to form *N and was oxidized to $*CO_2$. The adsorbed *CO also facilitated the subsequent hydrogenation of *N to $*NH_2$, which could be coupled to $*CONH_2$ and produce urea. Overall, this work discloses that spatial management of *CO could tune the C−N coupling rate for urea synthesis during coelectrolysis of CO_2 and NO_3^-.

In summary, a unique stacked tandem GDE was designed for electrocatalytic urea synthesis from cascaded CO_2 and NO_3^- reduction on dual-active catalytic sites. The local $*\theta_{CO}$ on the Cu CL was increased by tailoring the area of the CO-selective ZnO site, which promotes the NO_3^- reduction to $*NH_2$ and thus accelerates the C−N coupling rate for urea synthesis. Remarkably, the stacked $Cu_{1.0}/ZnO_{0.5}$ GDE with an optimal CL area ratio achieved a high urea yield of 3.2 μmol h^{-1} cm^{-2} and a high FE of 37.4% at −0.3 V. This work provides an effective strategy to boost the cascade electrocatalytic C−N coupling reaction kinetics beyond catalyst design.

■ ASSOCIATED CONTENT

Supporting Information

The Supporting Information is available free of charge at https://pubs.acs.org/doi/10.1021/acsenergylett.3c00824.

Experimental section, SEM and EDS mapping images, UV−vis spectra, urea yield and FE data, EIS spectra, in situ Raman spectra, in situ ATR-FTIR spectra, XRD patterns, XPS spectra, and Table S1 (PDF)

■ AUTHOR INFORMATION

Corresponding Authors

Jianfang Zhang − *School of Materials Science and Engineering, Hefei University of Technology, Hefei 230009, China;* orcid.org/0000-0002-3870-4906; Email: jfzhang@hfut.edu.cn

Jingjie Wu − *Department of Chemical and Environmental Engineering, University of Cincinnati, Cincinnati, Ohio 45221, United States;* orcid.org/0000-0001-6617-0895; Email: wu2jj@ucmail.uc.edu

Yucheng Wu − *School of Materials Science and Engineering, Hefei University of Technology, Hefei 230009, China; Key Laboratory of Advanced Functional Materials and Devices of Anhui Province, Hefei University of Technology, Hefei 230009, China;* orcid.org/0000-0002-1549-0546; Email: ycwu@hfut.edu.cn

Authors

Yan Wang − *School of Materials Science and Engineering, Hefei University of Technology, Hefei 230009, China;* orcid.org/0000-0003-1479-1715

Shuai Xia − *School of Materials Science and Engineering, Hefei University of Technology, Hefei 230009, China*

Zhengyuan Li − *Department of Chemical and Environmental Engineering, University of Cincinnati, Cincinnati, Ohio 45221, United States*

Rui Cai − *School of Materials Science and Engineering, Hefei University of Technology, Hefei 230009, China*

Cuiping Yu − *School of Materials Science and Engineering, Hefei University of Technology, Hefei 230009, China*

Yong Zhang − *School of Materials Science and Engineering, Hefei University of Technology, Hefei 230009, China;* orcid.org/0000-0002-7625-2234

Complete contact information is available at: https://pubs.acs.org/10.1021/acsenergylett.3c00824

Author Contributions

‖Y.W. and S.X. contributed equally.

Notes

The authors declare no competing financial interest.

■ ACKNOWLEDGMENTS

We acknowledge the support from National Natural Science Foundation of China (Grants 52202226, 52172293, and 52072106), Key R&D Projects of Anhui Province (Grant 202104b11020016), China Postdoctoral Science Foundation (Grant 2021M701028), and Natural Science Foundation of Anhui Province (Grant 2108085QB66). We also acknowledge the financial support from the Fundamental Research Funds for the Central Universities (Grants JZ2021HGQB0282, PA2021GDSK0088 and PA2022GDSK0056, PA2022GDSK0050) and the 111 Project (Grant B18018).

J.W. thanks the support from Natural Science Foundation (Award CBET-2033343).

REFERENCES

(1) Zhu, X.; Zhou, X.; Jing, Y.; Li, Y. Electrochemical Synthesis of Urea on MBenes. *Nat. Commun.* **2021**, *12* (1), 4080.
(2) Yuan, M.; Zhang, H.; Xu, Y.; Liu, R.; Wang, R.; Zhao, T.; Zhang, J.; Liu, Z.; He, H.; Yang, C.; Zhang, S.; Zhang, G. Artificial Frustrated Lewis Pairs Facilitating the Electrochemical N_2 and CO_2 Conversion to Urea. *Chem. Catal* **2022**, *2* (2), 309−320.
(3) Meessen, J. Urea synthesis. *Chem. Ing. Technol.* **2014**, *86* (12), 2180−2189.
(4) Comer, B. M.; Fuentes, P.; Dimkpa, C. O.; Liu, Y.-H.; Fernandez, C. A.; Arora, P.; Realff, M.; Singh, U.; Hatzell, M. C.; Medford, A. J. Prospects and Challenges for Solar Fertilizers. *Joule* **2019**, *3* (7), 1578−1605.
(5) Li, D.; Zhao, Y.; Miao, Y.; Zhou, C.; Zhang, L. P.; Wu, L. Z.; Zhang, T. Accelerating Electron-Transfer Dynamics by TiO_2-Immobilized Reversible Single-Atom Copper for Enhanced Artificial Photosynthesis of Urea. *Adv. Mater.* **2022**, *34*, No. 2207793.
(6) Bharath, G.; Karthikeyan, G.; Kumar, A.; Prakash, J.; Venkatasubbu, D.; Kumar Nadda, A.; Kumar Gupta, V.; Abu Haija, M.; Banat, F. Surface Engineering of Au Nanostructures for Plasmon-Enhanced Electrochemical Reduction of N_2 and CO_2 into Urea in the Visible-NIR Region. *Appl. Energy* **2022**, *318*, 119244.
(7) Chen, C.; Zhu, X.; Wen, X.; Zhou, Y.; Zhou, L.; Li, H.; Tao, L.; Li, Q.; Du, S.; Liu, T.; Yan, D.; Xie, C.; Zou, Y.; Wang, Y.; Chen, R.; Huo, J.; Li, Y.; Cheng, J.; Su, H.; Zhao, X.; Cheng, W.; Liu, Q.; Lin, H.; Luo, J.; Chen, J.; Dong, M.; Cheng, K.; Li, C.; Wang, S. Coupling N_2 and CO_2 in H_2O to Synthesize Urea Under Ambient Conditions. *Nat. Chem.* **2020**, *12* (8), 717−724.
(8) Chen, C.; He, N.; Wang, S. Electrocatalytic C−N Coupling for Urea Synthesis. *Small Sci.* **2021**, *1* (11), 2100070.
(9) Kayan, D. B.; Köleli, F. Simultaneous Electrocatalytic Reduction of Dinitrogen and Carbon Dioxide on Conducting Polymer Electrodes. *Appl. Catal. B: Environ.* **2016**, *181*, 88−93.
(10) Zhang, Z.; Guo, L. Electrochemical Reduction of CO_2 and N_2 to Synthesize Urea on Metal-Nitrogen-Doped Carbon Catalysts: A Theoretical Study. *Dalton. Trans.* **2021**, *50* (32), 11158−11166.
(11) Fu, J.; Yang, Y.; Hu, J.-S. Dual-Sites Tandem Catalysts for C−N Bond Formation via Electrocatalytic Coupling of CO_2 and Nitrogenous Small Molecules. *ACS Mater. Lett.* **2021**, *3*, 1468−1476.
(12) Huang, Y.; Yang, R.; Wang, C.; Meng, N.; Shi, Y.; Yu, Y.; Zhang, B. Direct Electrosynthesis of Urea from Carbon Dioxide and Nitric Oxide. *ACS Energy Lett.* **2022**, *7* (1), 284−291.
(13) Mukherjee, J.; Paul, S.; Adalder, A.; Kapse, S.; Thapa, R.; Mandal, S.; Ghorai, B.; Sarkar, S.; Ghorai, U. K. Understanding the Site-Selective Electrocatalytic Co-Reduction Mechanism for Green Urea Synthesis Using Copper Phthalocyanine Nanotubes. *Adv. Funct. Mater.* **2022**, *32*, 2200882.
(14) Yuan, M.; Chen, J.; Bai, Y.; Liu, Z.; Zhang, J.; Zhao, T.; Wang, Q.; Li, S.; He, H.; Zhang, G. Unveiling Electrochemical Urea Synthesis by Co-Activation of CO_2 and N_2 with Mott-Schottky Heterostructure Catalysts. *Angew. Chem., Int. Ed.* **2021**, *60* (19), 10910−10918.
(15) Lv, C.; Zhong, L.; Liu, H.; Fang, Z.; Yan, C.; Chen, M.; Kong, Y.; Lee, C.; Liu, D.; Li, S.; Liu, J.; Song, L.; Chen, G.; Yan, Q.; Yu, G. Selective Electrocatalytic Synthesis of Urea with Nitrate and Carbon Dioxide. *Nat. Sustain.* **2021**, *4*, 868−876.
(16) Liu, S.; Wang, M.; Cheng, Q.; He, Y.; Ni, J.; Liu, J.; Yan, C.; Qian, T. Turning Waste into Wealth: Sustainable Production of High-Value-Added Chemicals from Catalytic Coupling of Carbon Dioxide and Nitrogenous Small Molecules. *ACS Nano* **2022**, *16*, 17911−17930.
(17) Qin, B.; Li, Y. H.; Zhang, Q.; Yang, G.; Wang, H.; Zhang, Y.; Peng, F. Mechanistic Insights into the Electrochemical Reduction of CO_2 and N_2 on the Regulation of a Boron Nitride Defect-Derived Two-Dimensional Catalyst using Density Functional Theory Calculations. *J. Phys. Chem. Lett.* **2021**, *12* (30), 7151−7158.
(18) Wan, Y.; Xu, J.; Lv, R. Heterogeneous Electrocatalysts Design for Nitrogen Reduction Reaction under Ambient Conditions. *Mater. Today* **2019**, *27*, 69−90.
(19) Lv, C.; Lee, C.; Zhong, L.; Liu, H.; Liu, J.; Yang, L.; Yan, C.; Yu, W.; Hng, H. H.; Qi, Z.; Song, L.; Li, S.; Loh, K. P.; Yan, Q.; Yu, G. A Defect Engineered Electrocatalyst that Promotes High-Efficiency Urea Synthesis under Ambient Conditions. *ACS Nano* **2022**, *16*, 8213−8222.
(20) Yuan, M.; Chen, J.; Xu, Y.; Liu, R.; Zhao, T.; Zhang, J.; Ren, Z.; Liu, Z.; Streb, C.; He, H.; Yang, C.; Zhang, S.; Zhang, G. Highly Selective Electroreduction of N_2 and CO_2 to Urea over Artificial Frustrated Lewis Pairs. *Energy Environ. Sci.* **2021**, *14* (12), 6605−6615.
(21) Saravanakumar, D.; Song, J.; Lee, S.; Hur, N. H.; Shin, W. Electrocatalytic Conversion of Carbon Dioxide and Nitrate Ions to Urea by a Titania-Nafion Composite Electrode. *ChemSusChem* **2017**, *10* (20), 3999−4003.
(22) Liu, S.; Yin, S.; Wang, Z.; Xu, Y.; Li, X.; Wang, L.; Wang, H. AuCu Nanofibers for Electrosynthesis of Urea from Carbon Dioxide and Nitrite. *Cell Rep. Phys. Sci.* **2022**, *3* (5), 100869.
(23) Siva, P.; Prabu, P.; Selvam, M.; Karthik, S.; Rajendran, V. Electrocatalytic Conversion of Carbon Dioxide to Urea on Nano-$FeTiO_3$ Surface. *Ionics* **2017**, *23* (7), 1871−1878.
(24) Wei, X.; Wen, X.; Liu, Y.; Chen, C.; Xie, C.; Wang, D.; Qiu, M.; He, N.; Zhou, P.; Chen, W.; Cheng, J.; Lin, H.; Jia, J.; Fu, X. Z.; Wang, S. Oxygen Vacancy-Mediated Selective C-N Coupling toward Electrocatalytic Urea Synthesis. *J. Am. Chem. Soc.* **2022**, *144* (26), 11530−11535.
(25) Leverett, J.; Tran-Phu, T.; Yuwono, J. A.; Kumar, P.; Kim, C.; Zhai, Q.; Han, C.; Qu, J.; Cairney, J.; Simonov, A. N.; Hocking, R. K.; Dai, L.; Daiyan, R.; Amal, R. Tuning the Coordination Structure of Cu-N-C Single Atom Catalysts for Simultaneous Electrochemical Reduction of CO_2 and NO_3^- to Urea. *Adv. Energy Mater.* **2022**, *12* (32), 2201500.
(26) Meng, N.; Huang, Y.; Liu, Y.; Yu, Y.; Zhang, B. Electrosynthesis of Urea from Nitrite and CO_2 over Oxygen Vacancy-rich ZnO Porous Nanosheets. *Cell Rep. Phys. Sci.* **2021**, *2* (3), 100378.
(27) Zhang, M. T.; Hammarstrom, L. Proton-Coupled Electron Transfer from Tryptophan: A Concerted Mechanism with Water as Proton Acceptor. *J. Am. Chem. Soc.* **2011**, *133* (23), 8806−9.
(28) Meng, N.; Ma, X.; Wang, C.; Wang, Y.; Yang, R.; Shao, J.; Huang, Y.; Xu, Y.; Zhang, B.; Yu, Y. Oxide-Derived Core-Shell Cu@Zn Nanowires for Urea Electrosynthesis from Carbon Dioxide and Nitrate in Water. *ACS Nano* **2022**, *16*, 9095−9104.
(29) Krzywda, P. M.; Rodríguez, A. P.; Benes, N. E.; Mei, B. T.; Mul, G. Carbon-Nitrogen Bond Formation on Cu Electrodes during CO_2 Reduction in NO_3^- Solution. *Appl. Catal. B: Environ.* **2022**, *316*, 121512.
(30) Liu, X.; Jiao, Y.; Zheng, Y.; Jaroniec, M.; Qiao, S. Z. Mechanism of C-N Bonds Formation in Electrocatalytic Urea Production Revealed by ab initio Molecular Dynamics Simulation. *Nat. Commun.* **2022**, *13* (1), 5471.
(31) Geng, J.; Ji, S.; Jin, M.; Zhang, C.; Xu, M.; Wang, G.; Liang, C.; Zhang, H. Ambient Electrosynthesis of Urea with Nitrate and Carbon Dioxide over Iron-Based Dual-Sites. *Angew. Chem., Int. Ed.* **2023**, *62*, No. 202210958.
(32) Feng, Y.; Yang, H.; Zhang, Y.; Huang, X.; Li, L.; Cheng, T.; Shao, Q. Te-Doped Pd Nanocrystal for Electrochemical Urea Production by Efficiently Coupling Carbon Dioxide Reduction with Nitrite Reduction. *Nano Lett.* **2020**, *20* (11), 8282−8289.
(33) Huang, Y.; Handoko, A. D.; Hirunsit, P.; Yeo, B. S. Electrochemical Reduction of CO_2 Using Copper Single-Crystal Surfaces: Effects of CO* Coverage on the Selective Formation of Ethylene. *ACS Catal.* **2017**, *7* (3), 1749−1756.
(34) Li, J.; Wang, Z.; McCallum, C.; Xu, Y.; Li, F.; Wang, Y.; Gabardo, C. M.; Dinh, C.-T.; Zhuang, T.-T.; Wang, L.; Howe, J. Y.; Ren, Y.; Sargent, E. H.; Sinton, D. Constraining CO Coverage on Copper Promotes High-Efficiency Ethylene Electroproduction. *Nat. Catal.* **2019**, *2* (12), 1124−1131.

https://doi.org/10.1021/acsenergylett.3c00824
ACS Energy Lett. 2023, 8, 3373−3380

(35) Zhang, J.; Tian, Y.; Zhang, T.; Li, Z.; She, X.; Wu, Y.; Wang, Y.; Wu, J. Confinement of Intermediates in Blue TiO_2 Nanotube Arrays Boosts Reaction Rate of Nitrogen Electrocatalysis. *ChemCatChem* **2020**, *12* (10), 2760−2767.
(36) Yuan, M.; Chen, J.; Bai, Y.; Liu, Z.; Zhang, J.; Zhao, T.; Shi, Q.; Li, S.; Wang, X.; Zhang, G. Electrochemical C-N Coupling with Perovskite Hybrids toward Efficient Urea Synthesis. *Chem. Sci.* **2021**, *12* (17), 6048−6058.
(37) Liu, X.; Kumar, P. V.; Chen, Q.; Zhao, L.; Ye, F.; Ma, X.; Liu, D.; Chen, X.; Dai, L.; Hu, C. Carbon Nanotubes with Fluorine-Rich Surface as Metal-Free Electrocatalyst for Effective Synthesis of Urea from Nitrate and CO_2. *Appl. Catal. B: Environ.* **2022**, *316*, 121618.
(38) Cao, N.; Quan, Y.; Guan, A.; Yang, C.; Ji, Y.; Zhang, L.; Zheng, G. Oxygen Vacancies Enhanced Cooperative Electrocatalytic Reduction of Carbon Dioxide and Nitrite Ions to Urea. *J. Colloid Interface Sci.* **2020**, *577*, 109−114.
(39) She, X.; Zhang, T.; Li, Z.; Li, H.; Xu, H.; Wu, J. Tandem Electrodes for Carbon Dioxide Reduction into C_{2+} Products at Simultaneously High Production Efficiency and Rate. *Cell Rep. Phys. Sci.* **2020**, *1* (4), 100051.
(40) Zhang, T.; Li, Z.; Zhang, J.; Wu, J. Enhance CO_2-to-C_{2+} Products Yield through Spatial Management of CO Transport in Cu/ZnO Tandem Electrodes. *J. Catal.* **2020**, *387*, 163−169.
(41) Zhang, T.; Bui, J. C.; Li, Z.; Bell, A. T.; Weber, A. Z.; Wu, J. Highly Selective and Productive Reduction of Carbon Dioxide to Multicarbon Products via in situ CO Management Using Segmented Tandem Electrodes. *Nat. Catal.* **2022**, *5* (3), 202−211.
(42) Zhang, Y.; Wang, Y.; Han, L.; Wang, S.; Cui, T.; Yan, Y.; Xu, M.; Duan, H.; Kuang, Y.; Sun, X. Nitrite Electroreduction to Ammonia Promoted by Molecular Carbon Dioxide with Near-unity Faradaic Efficiency. *Angew. Chem., Int. Ed.* **2023**, *62* (3), No. e202213711.
(43) Luo, W.; Zhang, Q.; Zhang, J.; Moioli, E.; Zhao, K.; Züttel, A. Electrochemical Reconstruction of ZnO for Selective Reduction of CO_2 to CO. *Appl. Catal. B: Environ.* **2020**, *273*, 119060.
(44) Xiang, Q.; Li, F.; Wang, J.; Chen, W.; Miao, Q.; Zhang, Q.; Tao, P.; Song, C.; Shang, W.; Zhu, H.; Deng, T.; Wu, J. Heterostructure of ZnO Nanosheets/Zn with a Highly Enhanced Edge Surface for Efficient CO_2 Electrochemical Reduction to CO. *ACS Appl. Mater. Interfaces* **2021**, *13* (9), 10837−10844.
(45) Wang, Y.; Zhou, W.; Jia, R.; Yu, Y.; Zhang, B. Unveiling the Activity Origin of a Copper-based Electrocatalyst for Selective Nitrate Reduction to Ammonia. *Angew. Chem., Int. Ed.* **2020**, *59* (13), 5350−5354.
(46) Chen, G.-F.; Yuan, Y.; Jiang, H.; Ren, S.-Y.; Ding, L.-X.; Ma, L.; Wu, T.; Lu, J.; Wang, H. Electrochemical Reduction of Nitrate to Ammonia via Direct Eight-Electron Transfer Using a Copper−Molecular Solid Catalyst. *Nat. Energy* **2020**, *5* (8), 605−613.
(47) Takagi, N.; Ishimura, K.; Miura, H.; Shishido, T.; Fukuda, R.; Ehara, M.; Sakaki, S. Catalysis of Cu Cluster for NO Reduction by CO: Theoretical Insight into the Reaction Mechanism. *ACS Omega* **2019**, *4* (2), 2596−2609.
(48) Yuan, M.; Chen, J.; Zhang, H.; Li, Q.; Zhou, L.; Yang, C.; Liu, R.; Liu, Z.; Zhang, S.; Zhang, G. Host−Guest Molecular Interaction Promoted Urea Electrosynthesis over a Precisely Designed Conductive Metal−Organic Framework. *Energy Environ. Sci.* **2022**, *15* (5), 2084−2095.
(49) Qin, J.; Liu, N.; Chen, L.; Wu, K.; Zhao, Q.; Liu, B.; Ye, Z. Selective Electrochemical Urea Synthesis from Nitrate and CO_2 Using In Situ Ru Anchoring onto a Three-Dimensional Copper Electrode. *ACS Sustain. Chem. Eng.* **2022**, *10* (48), 15869−15875.
(50) Butcher, D. P.; Gewirth, A. A. Nitrate Reduction Pathways on Cu Single Crystal Surfaces: Effect of Oxide and Cl^-. *Nano Energy* **2016**, *29*, 457−465.
(51) Chen, K.; Zhang, X.; MacFarlane, D. R. Ultrasensitive Surface-Enhanced Raman Scattering Detection of Urea by Highly Ordered Au/Cu Hybrid Nanostructure Arrays. *Chem. Commun.* **2017**, *53* (56), 7949−7952.
(52) Chen, X.; Sun, C.; Wu, S.; Xue, D. Nucleation-Dependant Chemical Bonding Paradigm: the Effect of Rare Earth Ions on the Nucleation of Urea in Aqueous Solution. *Phys. Chem. Chem. Phys.* **2017**, *19* (13), 8835−8842.
(53) Yao, Y.; Zhu, S.; Wang, H.; Li, H.; Shao, M. A Spectroscopic Study on the Nitrogen Electrochemical Reduction Reaction on Gold and Platinum Surfaces. *J. Am. Chem. Soc.* **2018**, *140* (4), 1496−1501.

https://doi.org/10.1021/acsenergylett.3c00824
ACS Energy Lett. 2023, 8, 3373−3380